2007-05-03

Multi-stable Compliant Rolling-contact Elements

Peter Andrew Halverson
Brigham Young University - Provo

MULTI-STABLE COMPLIANT ROLLING-CONTACT ELEMENTS

by

Peter Andrew Halverson

A thesis submitted to the faculty of

Brigham Young University

in partial fulfillment of the requirements for the degree of

Master of Science

Department of Mechanical Engineering

Brigham Young University

August 2007

BRIGHAM YOUNG UNIVERSITY

GRADUATE COMMITTEE APPROVAL

of a thesis submitted by

Peter Andrew Halverson

This thesis has been read by each member of the following graduate committee and by majority vote has been found to be satisfactory.

Date	Larry L. Howell, Chair
Date	Brian D. Jensen
Date	Spencer P. Magleby

BRIGHAM YOUNG UNIVERSITY

As chair of the candidate's graduate committee, I have read the thesis of Peter Andrew Halverson in its final form and have found that (1) its format, citations, and bibliographical style are consistent and acceptable and fulfill university and department style requirements; (2) its illustrative materials including figures, tables, and charts are in place; and (3) the final manuscript is satisfactory to the graduate committee and is ready for submission to the university library.

Date

Larry L. Howell
Chair, Graduate Committee

Accepted for the Department

Matthew R. Jones
Graduate Coordinator

Accepted for the College

Alan R. Parkinson
Dean, Ira A. Fulton College of
Engineering and Technology

ABSTRACT

MULTI-STABLE COMPLIANT ROLLING-CONTACT ELEMENTS

Peter Andrew Halverson

Department of Mechanical Engineering

Master of Science

The purpose of this research is the development of design concepts and models of large-angle, compliant, multistable, revolute joints. This research presents evidence of the capability of these models and concepts by presenting a case study in which the miniaturization of revolute joints are examined. Previous attempts at multistable revolute joints can be categorized into two categories: compliant and non-compliant mechanisms. Non-compliant multistable revolute joints are typified by a combination of pin-in-slot joints, springs, and detents. Due to factors inherit in design, non-compliant joints often succumb to friction, wear, and undesirable motion, that leads to a decline in performance. Compliant multistable joints, such as those discussed in this work, negate these issues by allowing deflection in one or more of their members. However, compliant mechanisms have challenges associated with large-angle revolutions, stress concentration, and, historically, they perform poorly in compression. The literature has been lacking information on the fabrication of compliant multistable revolute joints having more than two stable positions.

This work develops a truly multistable compliant revolute joint that is capable of multiple stable positions, the multistable compliant rolling-contact element

(CORE). A CORE is a contact-aided complaint mechanism that eliminates friction and wear by allowing two surfaces to roll on each other. Furthermore, the contact eliminates problems such as poor performance in compression, typically associated with compliant mechanisms. The device uses minima in potential energy to achieve multi-stability, through one of six mechanisms. The use of minima in the potential energy eliminates the need for detents and other fatigue prone devices. Multistability may be achieved by placing the CORE flexure into tension or using flexible segments attached to the foci; or by changing the initial curvature of the flexure, curvature of the CORE surface, cross sectional area of the flexure (both protagonistically or antagonistically), or material properties. The stability methods are evaluated via a Pugh scoring matrix and the most promising concept, stability through tension in the CORE flexures, examined further. The utility of mathematical models, developed in this work, that predict stress, strain, and activation force, are demonstrated via a case study. This work also demonstrates that the device is capable of large angle deflections (360°) and that the provided models permit efficient engineering design with COREs.

ACKNOWLEDGMENTS

There's an old saying that says it takes a village to raise a child. If this is true it takes a small army to write a thesis. I have received much help throughout the entire process. I would like to thank my Heavenly Father for his insight into the problem at hand; many prayers went into this research, and I could not have completed it without the answers that I received.

I would also like to thank my earthly parents, their emphasis on education is part of the reason I am where I am. Dr. Howell was a great mentor and friend by whose guidance I was able to learn a great deal. I would also like to thank my graduate committee members Drs Jensen and Magleby who were always available for discussions. Brian Winder and Joey Jacobsen for their aid in prototyping and assembly of the devices.

Lastly I would like to thank my wife Jennifer who has been a great support, and without whom I don't believe I would have ever gotten around to writing anything.

This work was funded in part by the Nokia Research Center, Dallas, TX.

Table of Contents

List of Tables

List of Figures

Chapter 1

Introduction

1.1 Purpose of This Research

Traditional pin-in-slot type hinges permit relative rotation between two rigid bodies. Problems arise in these mechanisms as the clearance between the pin and the slot introduce undesirable motion into the system, decreasing both precision and accuracy. These problems are compounded after time as the pin slides in the slot producing wear, thus increasing the clearance and further compounding the problem. Currently, in large scale devices, there are two remedies to reduce wear in a pin-in-slot type joint: (1) lubrication and (2) bearings.

By lubricating the joint, the designer introduces a thin film into the system, which provides a barrier between the two surfaces, reducing the coefficient of friction. The film effectively reduces the wear on the system, as it reduces the forces between the surfaces. The drawback of lubricated systems is that they require that the lubrication is replaced as it degrades by evaporation, or particles become entrained in the lubrication. Lubrication is generally undesirable in consumer devices as it is difficult to insure that a consumer will properly lubricate the device, thus the device may succumb to premature failure.

Bearings can also be used to reduce wear in joints. Bearings provide a third surface on which both surfaces roll. This motion reduces sliding and therefore wear is also reduced. However, even with the implementation of bearings, wear is still present and will often assume the form of fretting. A difficulty arises in design with bearings in that as bearings are added to the system they increase the part count thus increasing the manufacturing and assembly costs. Furthermore, bearings take up space inside the device and can only be manufactured to certain sizes and tolerances before costs

become prohibitive. These manufacturing limitations are contradictory to the current trend in consumer electronics: miniaturization.

There has been much focus in recent years in the miniturization of electronic devices. As semiconductor technology advances and it becomes increasingly easier and cheaper to place more and more transistors on a single chip, consumers are seeking these smaller more efficient devices. One of the major limitations to current electronic technology is the design of the hinge in foldable electronic devices. The current practice in consumer electronics is to use a pin-in-slot type hinge. Often times these devices, laptops, PDAs, cellphones, and the like, are in fact multi-stable devices.

A multi-stable device is any device that contains multiple stable positions. There are many devices that require, both compact storage and stability in both their stored and open positions, this is typically done today via a cam and spring. As these devices are miniaturized the spring and cam surfaces that enable the multiple stable positions in today's devices will have to be rethought and redesigned, as current technology will not permit efficient miniaturization. The need for a device that exhibits both multiple stable positions and a reduction in friction is great in the field of consumer electronics.

The purpose of this research is to investigate and develop design approaches for a novel compliant mechanism that is capable of large angle deflections, has the ability to retain several positions without any external stabilizing force, and that contains minimal volume and parts.

1.2 Outline of the Thesis

The remainder of this chapter is dedicated to work that has been performed by previous researchers. This includes a literature review and a discussion of the terminology used in the remainder of the thesis. Chapter 2 contains a discussion on the contributing factors to multiple stable positions in Compliant Rolling-contact Elements (CORE). Chapter 3 includes an in-depth study on one of the most promising categories of multi-stable CORE, tension-based stability. The final chapter includes

a summary of the research presented, and recommendations for further research into multi-stable CORE.

1.3 Terminology and Background

1.3.1 Adaptive Systems

There are many devices that require multiple stable positions. These devices implement what is known as an adaptive system. Adaptive systems have the ability to retain an altered position or multiple altered positions. Traditional adaptive systems achieve this through either an external force or friction to retain the system in its altered position(s). Problems arise in these systems in that they are either costly, from an energy standpoint, or the friction that is used to retain the system in its altered position(s) leads to wear and an eventual decrease in performance. Detents are an example of a common approach of adaptive systems and suffer from several of the problems typical to these systems, paticularly wear and degradation of performance over time.

Multi-stable mechanisms offer energy efficient, wear resistant solutions to adaptive systems [1, 2]. Multi-Stable Equilibrium Systems (MSE) differ from traditional adaptive systems in that they use a minimum in potential energy to obtain stability. As a result, they reduce the energy required for operation by remaining in one of their biased positions, even when all external forces are removed.

The cause of stability in MSE is easily explained using the "Ball on the Hill Analogy," as illustrated in Figure 1.1 [3]. When the ball is rolled up the hill its potential energy increases. When released, the ball will role downhill decreasing its potential energy. At the bottom of the trough (A or C) the potential energy is lower than the surroundings and the system is said to be in stable equilibrium because a small external disturbance only causes the system to oscillate around its current position [4]. Likewise, a system is said to be in unstable equilibrium (B) if a small external disturbance causes the system to diverge from its position. The system is considered neutrally stable (D) if, when exposed to a small external disturbance, the system's potential energy does not deviate from its initial value.

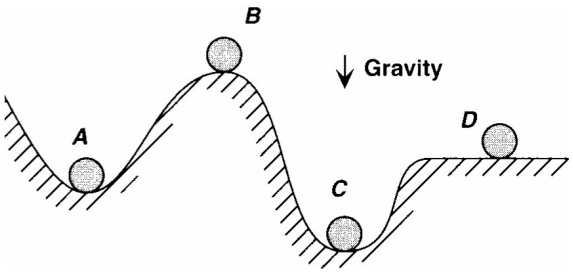

Figure 1.1: Ball on the hill analogy.

1.3.2 Compliant Mechanisms

A mechanism is any device that transfers or transforms motion or energy [5,6]. A compliant mechanism is any mechanism that transfers or transforms motion or energy through the deflection of one or more of its members. Compliant mechanisms can be used to replace typical rigid-body mechanisms. Furthermore, compliant mechanisms potentially provide motion with reduced wear, friction, and manufacturing costs over traditional rigid-body mechanisms [3]. These attributes, and their ability to store energy through the deflection of flexures, make them potential candidates for improved multi-stable mechanisms. Large-displacement compliant revolute joints, however, need to be designed to resist failure in torsion and compression, and to eliminate any high stress concentrations [7].

1.3.3 Bernoulli-Euler Theory

In 1744 Leonhard Euler published his theory "Methodus Inveniendi Leneas Curvas Maximi Minimive Peoprietate Gavdentes [8]." The theory stated simply that the moment in a long slender beam is proportional to the curvature, or

$$M = EI\frac{d\theta}{ds} \tag{1.1}$$

where E is the modulus of elasticity, I is the moment of inertia and $\frac{d\theta}{ds}$ is the curvature. He assumed that: 1) the material is linearly elastic, isotropic, and homogeneous; 2) the bending component of deflection is dominant. This equation and its assumptions

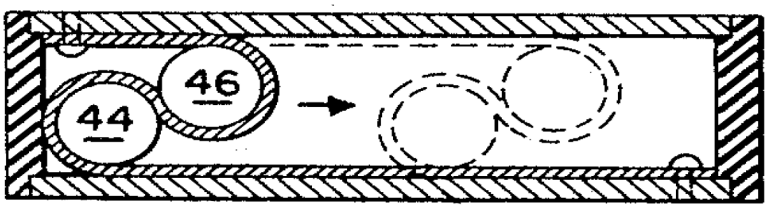

Figure 1.2: Donald Wilkes' Rolamite [10]

led to the development of modern-day force-deflection relationship by assuming small deflections by approximating the curvature by the second derivative of y with respect to x.

However when the beam is sufficiently thin enough that the neutral axis is coincident with the geometric centroidal axis, even when the beam is initially curved [3], equation (1.1) can be approximated as

$$M = \frac{EI}{R'} \tag{1.2}$$

where R' is the effective radius of curvature. Thus, if a flexure is thin and constrained to a surface with a prescribed curvature, the moment may be calculated and the stress determined.

1.4 Literature Review

Donald Wilkes of Sandia National Labs reported in 1967 on a device known as the "Rolamite" [9]. A band was wound, in one direction, around two cylindrical rollers ensuring a no-slip condition. One end of the band was attached to an upper plate and the other end to the lower, the plates were then arranged in such a fashion as to insure that the rollers could not be removed from the system (see Figure 1.2).

This mechanism allowed for the linear translation of the plates with minimum friction. Wilkes furthered his research by reporting that the force could be varied. This was done by changing the cross section of the Rolamite bands [9] [10]. Chironis

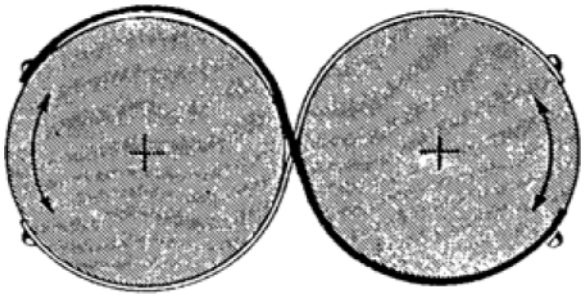

Figure 1.3: "Cross-strip rolling pivot", a CORE precursor [11]

and Sclater also reported a "cross-strip rolling pivot" showing that the pivot could be used on both Cylindrical- Cylindrical elements (Figure 1.3) and Cylindrical-Planar elements [11].

In their coetaneous work Cannon et al. [12, 13] and Jeanneau et al. [14] have shown that the use of "cross-strip rolling pivots" or COmpliant Rolling-contact Elements (CORE), as large displacement angular joints, eliminates stress concentrations and provides for large angular deflection that is resistant to off axis loads. Furthermore, they have shown that these mechanisms may be designed to produce a one-directional restoring torque, similar to that of a torsional spring. CORE mechanisms consist of two rigid objects which roll on each other. Compliant segments between the two objects insure a no-slip condition much like the teeth on gears.

The first analytical models of CORE mechanisms were developed independently by Jeanneau et al. [14] and Cannon et al. [13]. Jeanneau reported the stresses throughout the band experienced by two symmetric cylindrical rollers in two cases. The first case was a band without an initial curvature, the second was the band with an initial curvature of one of the CORE (referred to as the X_r joint by Jeanneau et al.) surfaces as fabricated via rapid prototyping. The result was a neutrally stable mechanism or a uni-stable mechanism.

Cannon et al. reported on analytical models dealing with both the stresses and the returning torques. As Cannon's models are essential to the current discussion, his models shall be briefly discussed in section 2.1, where the complete derivation of

the models can be found in his work. The curvature of the CORE beam is directly related to the curvature of the CORE surface at the point of contact.

Trease et al. introduced a design criteria for various large-displacement compliant joints [7]. The criteria stated that the joint must provide (1) a large range of motion, (2) minimal "axis drift" (3) increased off-axis stiffness, and (4) an avoidance of stress concentrations. COmpliant Rolling-contact Elements (CORE) have been shown to fulfil this criteria [13,14]. CORE mechanisms reduce wear and friction by allowing the surfaces to roll on each-other, creating a contact aided mechanism [15–18]. Furthermore, CORE mechanisms eliminate high stress concentrations and resist both off-axis, and compressive forces, that present difficulties in most large-angle compliant revolute joints, by constraining the radius of the flexible segment, thus constraining the stress [12–14].

Chapter 2

Design Principles

2.1 CORE Mechanism

A functional CORE mechanism consists of three or more CORE planes. Each plane consists of two rigid, curved surfaces connected by a flexible segment as shown in Figure 2.1. The CORE planes are then joined together in alternating directions (Figure 2.2) and assembled to bring the flexure in contact with the rigid surface. Such an assembly ensures that the surfaces stay in contact, as illustrated in Figure 2.3.

As the mechanism is displaced, the compliant flexure is transferred from one surface to the other and assumes the curvature of the mating surface, as shown in Figure 2.4. The flexure is fastened such that it insures a no-slip condition, much like the teeth on gears.

The Bernoulli-Euler equation states that the internal moment of a thin beam is directly proportional to the curvature of the beam. As the curvature of the flexure is directly related to the curvature of the mating CORE surface the internal moment, M, is expressed as

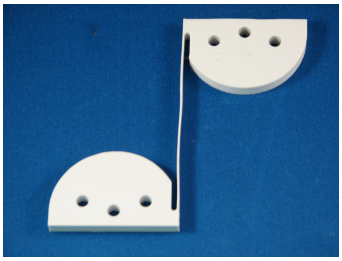

Figure 2.1: CORE plane with attached flexure

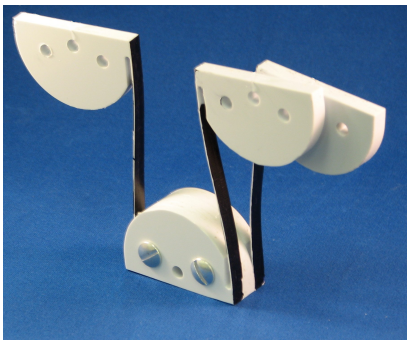

Figure 2.2: Partially assembled CORE mechanism

Figure 2.3: Assembled CORE mechanism

$$M = \frac{EI}{R'} \tag{2.1}$$

where E is the flexural modulus, I is the moment of inertia. R' is the effective radius of curvature and is calculated by

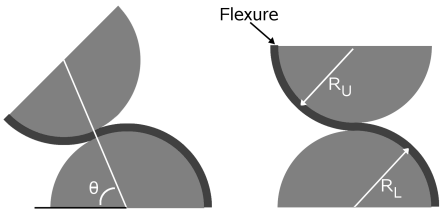

Figure 2.4: Movement of CORE mechanism (flexure thickness exaggerated)

$$R' = \left(\frac{1}{R_s} - \frac{1}{R_o} \right)^{-1} \tag{2.2}$$

where R_S is the radius of the constraining CORE surface and R_0 is the initial curvature of the CORE flexure, assuming that the thickness of the beam, h, is much less than R_s. For an initially straight CORE flexure, such as illustrated in Figure 2.3, $(R_0 = \infty)$ and $R' = R_s$.

The stress due to bending, σ, is

$$\sigma = \frac{Eh}{2R'} \tag{2.3}$$

The input torque required to maintain the CORE in a given position may be examined through a number of methods including: energy methods, numerical/FEA, or a free-body moment balance method [9]. The free-body moment balance method and a strain energy method are presented here because of the insight they provide. The free-body moment balance method is used to show the input torque required to maintain its position; stable positions will require no input torque. The strain energy method is used to distinguish the stable-equilibrium positions from the unstable equilibrium positions.

2.1.1 Free-body Method

As the CORE flexure transfers from one CORE surface to the other, the flexure passes an inflection point where the curvature changes instantaneously, thus the curvature of the flexure above the inflection point may be considered positive and the curvature below may be considered negative. The input torque is then determined by a free-body moment balance method:

$$T = \frac{E_U I_U}{R'_U} + \frac{E_L I_L}{R'_L} \tag{2.4}$$

where R'_U and R'_L are the upper and lower effective radii, respectively.

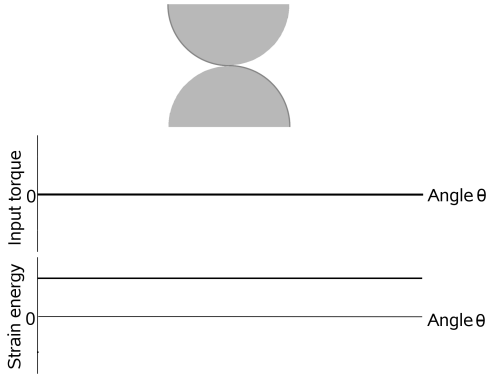

Figure 2.5: Stabilizing input torque and strain energy plots for a symmetric CORE

2.1.2 Strain-energy

The "Ball on the Hill Analogy" can be applied to the CORE system to find stable, unstable, and neutral equilibrium positions by identifying local maxima and local minima of strain energy. The strain energy, U, of a linear elastic deformation is related to the moment, M by:

$$\frac{dU}{ds} = \frac{M^2}{2EI} \tag{2.5}$$

Where ds is the arclength along the flexible segment, or $R_s d\theta$. The strain energy U is then calculated by substituting equation (2.1) into (2.5) and $ds = R_s d\theta$

$$U = \int \frac{EIR_s d\theta}{2R'^2} \tag{2.6}$$

Consider a basic CORE mechanism with $R_U = R_L$ as illustrated in Figure 2.4. A point along the flexure can be identified by the arclength measured along the flexible segment. The point of most interest is where the flexure intersects the line connecting the foci of R_U and R_L, as shown in Figure 2.4. This angle, θ, will be used as a nondimensional variable to identify this point and the position of the system. For the basic CORE shown in Figure 2.5, note that at any angle, θ, the internal moment in the flexure, to the right and left of the inflection point have equal magnitudes but opposite signs. Thus, their sum at any angle is zero and no input torque is required

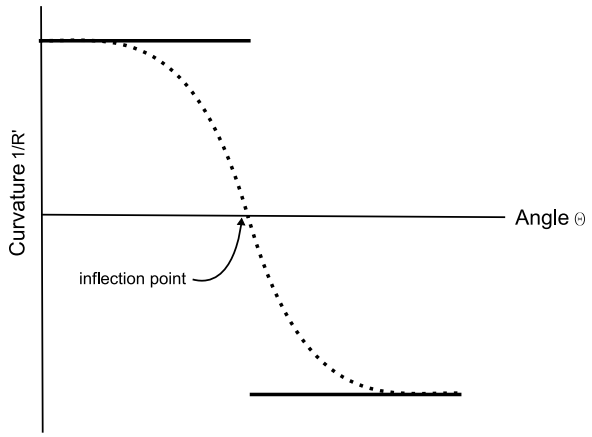

Figure 2.6: Change in curvature of flexure, $\frac{1}{R'}$, theoretical (solid) and actual (dotted)

to maintain any position, θ; the CORE mechanism of this configuration is neutrally stable.

The strain energy method verifies these results. Consider the CORE plane shown in Figure 2.5. The flexural modulus, E, and the moment of inertia, I, are constant throughout the flexure. The strain energy of the entire flexure, at any position θ may be calculated as

$$U = \frac{EI}{2}\int_0^{\theta}\frac{R_s d\theta}{R'^2} + \frac{EI}{2}\int_{\theta}^{\pi}\frac{R_s d\theta}{R'^2} \tag{2.7}$$

This results in the following constant energy for any angle θ

$$U = \frac{EIR_s\pi}{2R'^2} \tag{2.8}$$

Because the strain energy is constant, no input torque T is required for the system to retain its current position.

The change of curvature at the inflection point presents a unique difficulty in analysis. Theoretically as the flexure passes from one constraining surface to the other, the change in radius, from positive to negative, happens instantaneously (Figure 2.6), and in a symmetric CORE, such as illustrated in Figure 2.5, is neutrally stable. However, a discontinuity in moment would require infinite shear. As no material can make this possible, the moment must change gradually, as shown in Figure

2.6. In a symmetric CORE, both symmetric in surface as well as beam geometry, this still results in neutral stability, as the positive and negative moments change congruently. However, when the CORE is unsymmetric the input torque required for stability of a system will differ from the theoretical value. This difference may be reduced by placing the CORE flexures into tension, as the tensile stress will dominate the shear stress.

2.2 Stability Models

Multi-stable CORE mechanisms can be divided into two different classes: *bending stable* and *tension stable*. The stability of bending stable mechanisms, called such as they primarily derive their stability through the bending of the CORE flexure, are governed by equation (2.4). Tension stable mechanisms, called such as they primarily derive their stability by placing a member into tension, are governed by another set of equations, which are discussed in section 3.2. To facilitate the discussion of multi-stable CORE mechanisms, the radius of curvature of CORE surfaces R_U and R_L shall be considered circular, unless specifically noted otherwise. The principles discussed, however, are also applicable for elliptical CORE mechanisms.

2.2.1 Bending Stable

Equation (2.4) implies that the input torque may be varied by changing any one of several variables. The bending stable mechanisms are categorized by these possible characteristics:

1. Initial Curvature of the Flexure
2. Curvature of CORE Surface
3. Cross-Sectional Area of Flexure (protagonistic)
4. Cross-Sectional Area of Flexure (antagonistic)
5. Material Properties

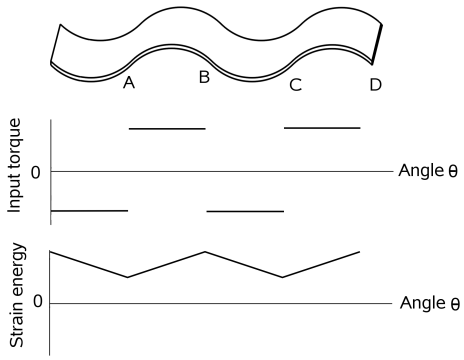

Figure 2.7: Topography of CORE flexure with varying initial curvature and plots of stabilizing input torque and strain energy

Although discussed separately here, bending stable techniques may be combined to increase the activation energy, (the minimum amount of energy required to move the system to its next stable position, or the height of the "hill" in the analogy) of the system and hence the overall stability. Each of the five principles are discussed in more detail next.

(1) *Change in Initial Curvature of the Flexure*: As stated in equation (2.1), the internal moment in the flexure is related to the effective radius of curvature of the flexure, R'. During manufacture the initial curvature of the flexure, R_0, may be varied along the flexure length. The magnitude and direction of these curvatures may also be made to vary as illustrated in Figure 2.7. Because the magnitude and direction of the initial curvatures, R_0, vary along the flexure length, the effective radius of curvature, R', and the internal moment will also vary along its length. Thus the input torque, T, as given in equation (2.4), also varies as the mechanism is displaced.

The flexure shown in Figure 2.7 is constructed with several initial curvatures of equal magnitude yet alternating signs, (it is unnecessary that the initial curvature of the flexure be equal to that of the CORE surface). The strain-energy graph indicates that positions A and C are stable equilibrium positions (local minimums of potential energy) and B and D are unstable equilibrium positions (local maximums of potential energy).

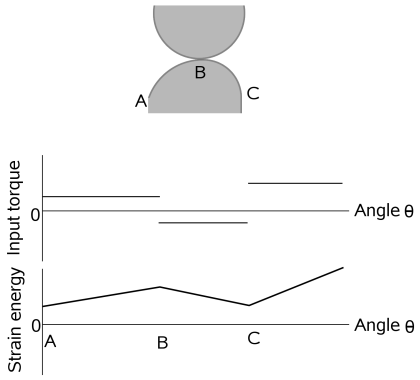

Figure 2.8: Stabilizing input torque and strain energy plots for a CORE with multiple surface curvatures

(2) *Change in Curvature of CORE Surface*: The second method of changing the effective radius R' is to change the radius of the constraining CORE surface. Assuming a constant area moment of inertia, I, and initial curvature, R_0, if the upper CORE surface is of a different curvature than the lower CORE surface i.e. $R_U \neq R_L$ a input torque will be required. This input torque may then be equalized by making $R_U = R_L$.

Figure 2.8 shows a CORE plane with changing radius, and an initially straight flexure. The upper radius R_U is constant and produces a constant moment. The lower radius begins at $R_L = 2R_U$, transitions to $R_L = \frac{R_U}{2}$, and then transitions to a flat surface (i.e. $R_L = \infty$). A graph of the strain-energy shows that positions A and C are stable equilibrium positions.

(3) *Change in Cross-Sectional Area of Flexure (Protagonistic)*: As the moment produced by the flexure is proportional to its second moment of inertia, I, a change in the cross sectional area of the CORE flexure may be used to induce stable regions or to change the input torque required for stability. As previously mentioned, the degree to which a change in area affects the input torque is dependent upon the amount of tension in the CORE flexure. A similar method was used in the Rolamite [9]. Many configurations of flexure are possible, such as the triangular, rectangular and circular cutouts shown in Figure 2.9. The thickness of the flexure may also be varied, which results in similar behavior.

Figure 2.9: Top down perspective of a CORE flexure with varied cross section

(4) *Change in Cross-Sectional Area of Flexure (Antagonistic)*: In case (2) it was shown that if $R_U \neq R_L$ a stabilizing input torque is needed to maintain position. Likewise in case (3) it was shown that the area moment of inertia, I, may be used to modify the required amount of stabilizing input torque. By combining case (2) and case (3), the input torque required for stability due to the difference in the area moments of inertia may cancel the input torque required due to the difference in the CORE radii. Although this method is not the most efficient method to produce stability in CORE mechanisms, it is helpful when the radii of curvature are fixed.

(5) *Change in Material Properties*: Changes in the flexural modulus along the length of the flexure will also result in a multi-stable CORE mechanism. This may be accomplished by varying the orientation of polymers through the placement of gates and channels, the addition of fillers such as glass in various parts of the flexure, orientation of fibers in a composite flexure, or a change in material at distinct points of the flexure.

2.2.2 Tension Stable

The approaches for achieving multi-stability described thus far have relied on the bending properties of the flexures. "Tension Stable" CORE devices place a member of the CORE mechanism in tension and exhibit the ability to form multi-stable CORE mechanisms with high activation energies. Tension is achieved by modifying the CORE geometry such that the flexures undergo different magnitudes of tension at varying angular displacements. The primary method of achieving multi-stability with a tension stable mechanism involves the cam and follower technique. In elliptical and circular CORE mechanisms the distance between the foci and the distance along the CORE surface typically do not change. Because these distances do not change,

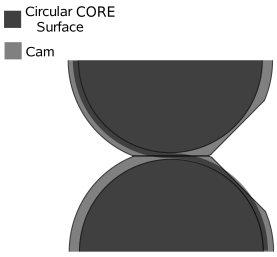

Figure 2.10: Tension-stable CORE in stable equilibrium

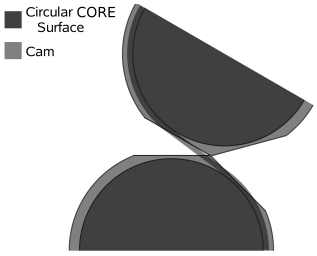

Figure 2.11: Tension-stable CORE in unstable equilibrium

the CORE mechanism can roll without slip. In the tension stable CORE, a cam and follower is placed parallel to the CORE mechanism, as shown in Figure 2.10 (the dark inner circle represents the CORE surface while the lighter outline represents the cam).

As the CORE mechanism rolls, the cam engages the follower, causing the CORE surfaces to separate, increasing the distance between the centers of the CORE surfaces (foci), as shown in Figure 2.11.

The variation in distance between the foci is then used to place the CORE into tension through one of two approaches: 1. placing the CORE flexures into tension and/or 2. joining the foci by an elastic element. The tension is released as the CORE rolls into its final position (Figure 2.12).

(1) *Placing the CORE flexures into tension*: In normal operation, both the distance between the foci and the distance traveled on the CORE surface is constant; thus the flexure length is also constant. As the distance between the foci is increased, the flexure length must increase in relation to the change in distance between the foci. This change in distance places the CORE flexures into tension, increasing the

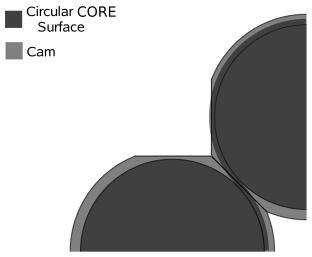

Figure 2.12: Tension-stable CORE in stable equilibrium

Table 2.1: Benchmarked stability methods (5 being the best)

Stability Method	Activation Energy	Size	Stable Positions	Failure Mode
Initial Curvature of flexure	3	3	4	Creep
Curvature of CORE Surface	2	1	1	Creep
Cross Sectional Area (Protagonistic)	1	4	5	Creep
Cross Sectional Area (Antagonistic)	1	4	4	Creep
Change in Material Prop	1	3	2	Creep
CORE Flexures into Tension	5	5	2	Fretting
Pinning the Foci	5	4	2	Fretting

strain energy of the system. As the cam is disengaged, the strain energy is released, creating stability in the CORE system, as illustrated in Figure 2.13.

(2) *Joining the Foci by an elastic element*: In addition to the stability generated by placing the CORE flexures into tension, stability may be further enhanced by

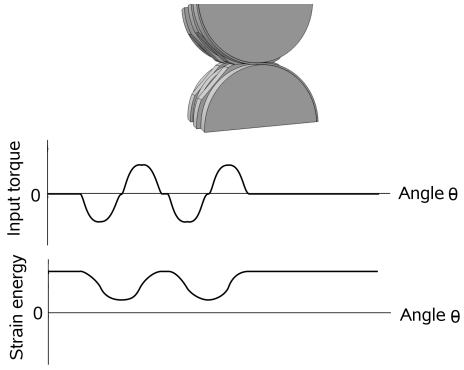

Figure 2.13: Tristable tension-stable CORE, stabilizing input torque and strain energy plots

placing an elastic element connecting the two foci. As the foci separate the element is placed into tension, thus increasing the overall strain energy of the system.

2.3 Comparison of Stability Methods

Several Methods for creating multi-stability in COmpliant Rolling-contact Elements (CORE) have been presented in this chapter. In this section the methods have been benchmarked against each other on a scale of one to five (one being the least desirable), as shown in Table 2.1. The categories that these methods were evaluated at were: activation energy, the minimum amount of energy required to switch the system from one stable position to the other; size, the degree in which system is able to be miniaturized using the selected method; number of stable positions, or the relative number of stable positions the system may have; and failure mode, which is the most likely mode of failure. Different stability methods may be desired for different applications.

Changes in the initial curvature of the flexure are beneficial in that it allows for a mechanism that has many stable postions, as the curvature of the flexure can be varied very rapidly. However, these mechanism are ill-suited for applications where a high degree of stability and compactness are both required, as stress and activation energy are linearly related. Also the flexures are much more susceptible to creep than tension stable methods.

Although changes to the cross sectional area of the beam allow for a large number of stable positions and may be compact, they do not require very much activation energy to switch from one stable position to the other. Furthermore, as the activation energy is affected by the tension in the flexures, these mechanisms may be difficult to design without extensive amounts of experimentation.

Affecting the stability of a CORE by changing the material properties will become more viable as better composite materials become available. Currently the use of this method is limited to CORE mechanims which require low activation energies, compactness and number of stable positions.

Tension stable methods, generally speaking, tend to allow for a greater activation energy and compactness than do bending stable methods. This phenomenon is due to the fact that the stress in tension based mechanisms is more evenly distributed than in bending stable mechanisms, where the stress varies linearly from the neutral axis. However, due to the design of the cam surface, these mechanisms are unable to produce a relatively high amount of stable postions. Thus these methods are good for generating a compact mechanism, with a high degree of stability, that only requires a few stable positions.

2.4 Conclusion

Seven distinct concepts have been presented that, when applied, result in multi-stability in CORE mechanisms. Multi-stability may be achieved by placing the CORE flexure into tension or using flexible segments attached to the foci; or by changing the initial curvature of the flexure, curvature of CORE surface, cross sectional area of the flexure (both protagonistically or antagonistically), or material properties. These concepts have expanded the application of CORE mechanisms and have been comparatively scored according to their stability, compactness, and number of stable positions and the likely mode of failure. The tension stable CORE has shown important advantages, and it is investigated in more detail in the next chapter.

Chapter 3

Tension stable CORE

The previous chapters introduced multi-stable CORE mechanism fundamental concepts. In the previous chapter a Pugh scoring matrix was used to evaluate the attributes of various stability techniques. This chapter presents models for the most promising concept: tension stable CORE mechanisms. The models are capable of determining stress, strain, and retaining forces and are derived using a strain-energy approach. Models are compared to empirical results and the utility of these models is demonstrated in a case study. The case study further indicates the fatigue properties of tension stable CORE.

Tension-stable CORE mechanisms can be constructed of three CORE planes and two cam and follower planes. Each CORE plane consists of two rigid, curved surfaces which roll on each other. A flexure joins the two surfaces together and when assembled is placed between the surfaces (see Figure 3.1). The CORE planes are then joined in alternating directions to insure that the surfaces stay in contact with the cam and follower planes, as illustrated in Figures 3.2 and 3.3. The flexure is fastened such that it insures a no-slip condition, much like the teeth on gears.

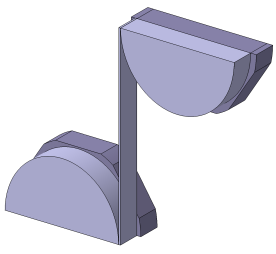

Figure 3.1: An unfolded CORE plane (foreground) with cam (background)

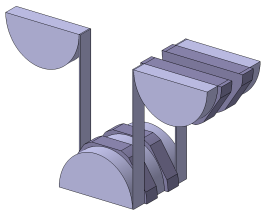

Figure 3.2: Unfolded CORE mechanism

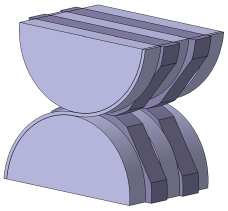

Figure 3.3: Assembled CORE mechanism

3.1 Guidelines for Cam Design

When the cam is not engaged, the compliant flexure is transferred from one surface to the other and assumes the curvature of the mating surface as shown in Figure 3.4. While the cam is in the "inactive" position(s) it behaves as a standard CORE mechanism and will exhibit neutral stability, assuming an initially straight beam and that the upper and lower CORE surfaces, R_U and R_L respectively are of the same radius (i.e. $R_U = R_L$). As the CORE mechanism is displaced and the cam is engaged, the CORE surface separates; placing the flexure in tension as illustrated in Figure 3.5.

Consider the exaggerated CORE shown in Figure 3.6. If the foci, F_U and F_L, are considered pinned to ground it becomes apparent that

$$\omega_U R_{DU} = V_1 = \omega_L R_{DL} \tag{3.1}$$

where R_{DU} and R_{DL} are the distances from the the contacting cam surface to the upper and lower CORE foci, and ω_U and ω_L are the angular velocities of the upper and

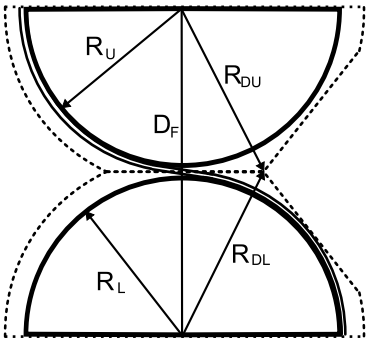

Figure 3.4: CORE mechanism in "inactive" position

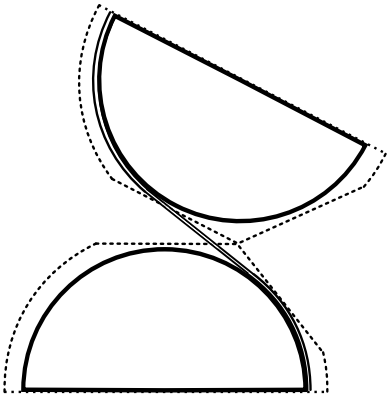

Figure 3.5: CORE mechanism in "active" position

lower surfaces respectively and V_1 is the tangential velocity at the contacting point. As the cam and the CORE surface have the same angular velocity a theoretical no slip condition holds when the connected CORE surfaces and the contacting cams have the same tangential velocity (Figure 3.6).

The relationship between the upper and lower cam radius and the upper and lower CORE surface radius is then expressed as

$$\frac{R_U}{R_L} = \frac{R_{DU}}{R_{DL}} \tag{3.2}$$

Some slip will occur as the flexure does not create a perfectly rigid connection between the CORE surfaces. This effect is examined more in detail later.

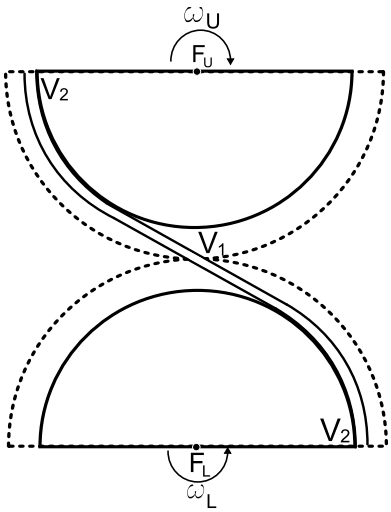

Figure 3.6: Velocity profiles of CORE (Cam surfaces exaggerated for illustration)

3.2 Modeling

When the cam is fully engaged, the distance between the two foci, D_F (referenced geometry shown in Figure 3.7), may be determined through the law of cosines as:

$$D_F = \sqrt{R_{DL}^2 + R_{DU}^2 - 2(R_{DU})(R_{DL}) \times \cos(\theta_{D_F})} \tag{3.3}$$

where the angle θ_{DF}, the angle between the sides R_{DL} and R_{DU}, is defined by

$$\theta_{D_F} = 180 - \theta_{R_{DU}} - \sin^{-1}\left(\frac{R_{DL}}{R_{DU}}\ \sin(\theta_{R_{DU}})\right) \tag{3.4}$$

and $\theta_{R_{DU}}$ is opposite of R_{DU} and is prescribed by

$$\theta_{R_{DU}} = \cos^{-1}\left(\frac{(R_U + R_L + h)^2 + R_{DL}^2 - R_{DU}^2}{2 \times (R_U + R_L + h)R_{DL}}\right) - \theta_1 \tag{3.5}$$

where θ_1 is the angle of rotation relative to the vertical axis. Due to its compliance, the flexible segment leaves both CORE surfaces in a tangential direction. The length of the flexure that is straight, L_S, may be calculated as

$$L_S = (R_U + R_L)\sqrt{\left(\frac{D_F}{R_U + R_L}\right)^2 - 1} \tag{3.6}$$

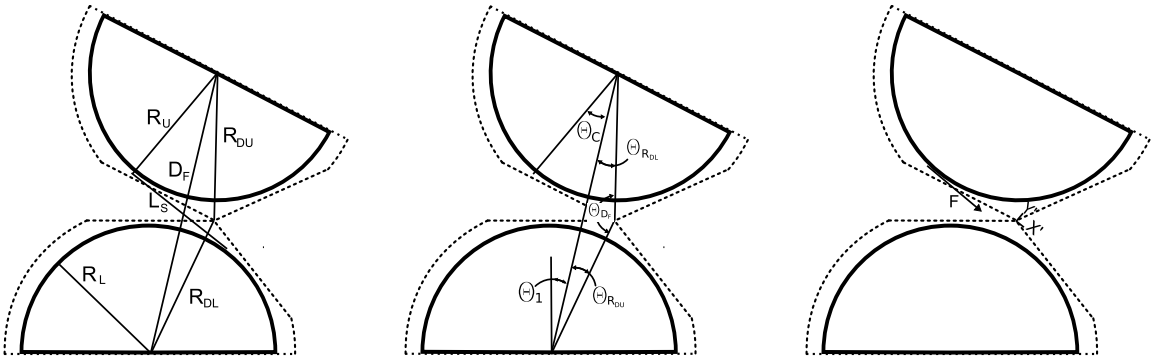

Figure 3.7: Referenced lines (left), angles (center), and forces (right) for tension stable CORE

The elongation that the flexure undergoes, E_L, is

$$E_L = L_S - (R_U + R_L)cos^{-1}\left(\frac{R_U + R_L}{D_F}\right) \tag{3.7}$$

or

$$E_L = (R_U + R_L)\left[\sqrt{\left(\frac{D_F}{R_U + R_L}\right)^2 - 1} - cos^{-1}\left(\frac{R_U + R_L}{D_F}\right)\right] \tag{3.8}$$

and the strain, ϵ, is:

$$\epsilon = \frac{E_L}{L_i} \tag{3.9}$$

where L_i is the initial length of the flexure. The strain energy of the system is expressed as

$$U = \frac{F^2 L_i}{2AE} \tag{3.10}$$

3.2.1 Stress Analysis

The stress due to tension, σ_T, is

$$\sigma_T = E\epsilon \tag{3.11}$$

where E is the modulus of elasticity. The stress due to bending, σ_B, is calculated as

$$\sigma_B = \frac{Eh}{2R_S} \tag{3.12}$$

Where h is the cross-sectional thickness.

3.2.2 Retaining Forces

The force generated in one flexure, F, is calculated from the stress as

$$F = \sigma_B A \tag{3.13}$$

where A is the cross-sectional area. Once the stress is known the retaining forces may be calculated using the free-body diagram shown in Figure 3.7, where

$$\theta_c = \sin\left(\frac{L_S}{D_F}\right) \tag{3.14}$$

The moment about the contact point is calculated for a flexure that is wrapped counter-clockwise and clockwise around the upper surface by constructing a new axis $x'y'$ about the contact point. The location where the flexible segment leaves the CORE surface on the $x'y'$ coordinate system is then determined by

$$A_{x'} = R_{DU} - R_U \cos(\theta_{R_{DL}} + \theta_C) \tag{3.15}$$

where $\theta_{R_{DL}}$ is the angle prescribed by

$$\theta_{R_{DL}} = 180 - \theta_{DF} - \theta_{R_{DU}} \tag{3.16}$$

$$A_{y'} = R_U \sin(\theta_{R_{DL}} + \theta_C) \tag{3.17}$$

The x' and y' of components of the force, $F_{x'}$ and $F_{y'}$ are

$$F_{x'} = -F \cos(\theta_{R_{DL}} + \theta_C) \tag{3.18}$$

$$F_{y'} = -F\sin(\theta_{R_{DL}} + \theta_C) \tag{3.19}$$

Thus the overall moment about the contacting point, due to the counter-clockwise wrapped flexure, M_{ccw}, is

$$\begin{aligned} M_{ccw} = &- (R_{DU} - R_U\cos(\theta_{R_{DL}} + \theta_C)) \times F\sin(\theta_{R_{DL}} + \theta_C) \\ &- R_U\sin(\theta_{R_{DL}} + \theta_C) \times F\cos(\theta_{R_{DL}} + \theta_C) \end{aligned} \tag{3.20}$$

Likewise the effect of the beams wound clockwise around the upper CORE surface can be found by

$$A_{x'} = R_{DU} - R_U\cos(\theta_{R_{DL}} - \theta_C) \tag{3.21}$$

$$A_{y'} = R_U\sin(\theta_{R_{DL}} - \theta_C) \tag{3.22}$$

The x' and y' of components of the force are

$$F_{x'} = -F\cos(\theta_{R_{DL}} - \theta_C) \tag{3.23}$$

$$F_{y'} = -F\sin(\theta_{R_{DL}} - \theta_C) \tag{3.24}$$

Thus the overall moment about the contacting point, due to the clockwise wrapped flexure, M_{cw} is

$$\begin{aligned} M_{cw} = &- (R_{DU} - R_U\cos(\theta_{R_{DL}} - \theta_C)) \times F\sin(\theta_{R_{DL}} - \theta_C) \\ &- R_U\sin(\theta_{R_{DL}} - \theta_C) \times F\cos(\theta_{R_{DL}} - \theta_C) \end{aligned} \tag{3.25}$$

And the total overall moment is simply the sum of M_{cw} and M_{ccw}. The unstable equilibrium point occurs when $\theta_c = 0$.

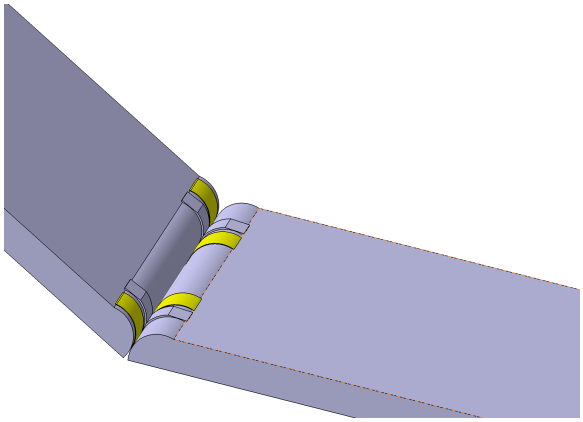

Figure 3.8: Small device case study showing a hinge for folding

3.3 Case Study

The utility of the models derived above may be illustrated by a case study. A hinge of a small device capable of folding, as shown in Figure 3.8, is used as the case study for this research. The device requires (1) a thickness, of less than 10mm, (2) a holding force, or the force that prevents the device from opening, of about 1.5 N, (3) a retaining force, or the force that prevents the device from closing, of about 2-3 N, and (4) stable position when closed and when opened to 150 degrees. In addition, the hinge needs to be designed for a fatigue life of at least 100,000 cycles to insure that the hinge would outlast the life of the device. Other constraints included symmetry of CORE surfaces and a small part count.

In order to determine the minimum size of the hinge, an optimization routine was implemented via OptdesX, using the above equations. The holding force was considered the tangential force located on the end of the device. The center of gravity, was considered to act on the midpoint of the device. Thus the input force, F_{in} was calculated as follows.

$$F_{in} = \frac{M_{ccw} + M_{cw}}{L} - \frac{1}{2}cos(\theta)W \tag{3.26}$$

where L and W are the length and weight of the device. As material selection for the flexure was key, several traditional metals were investigated as well as several

Table 3.1: Material comparison showing stresses for a 10mm CORE hinge

Material	σ_B (MPa)	σ_T (MPa)	σ_{Total} (MPa)
Steel	379	447	826
Aluminum	186	250	435
Titanium	216	363	579
Kevlar 29	3	278	281
Kevlar 49	3	317	320

Table 3.2: Specifications of CORE hinge

Specification	Value
Core Surface Radius	3.5 mm
Cam radius	3.71 mm
Flexure area	$4.4 * 10^{-7}\ mm^2$
Flexure length	1.6 mm
Unstable equilibrium Angle	29.5^o

polymers, and composite materials. The stresses for a 10mm (6.7 mm radius) CORE hinge that meets the above requirements are listed in Table 3.1. It is interesting to note that, due to the low modulus of elasticity of ABS, a hinge could not be constructed that fit all 4 requirements.

High bending stresses are expected for metals due to their high stiffness. As bending stresses do not contribute to the overall stability of tension stable CORE, anisotropic fibrous materials, such as Kevlar have been investigated. Ultimately Kevlar 49 was chosen for the construction of the physical prototype and fatigue testing due to its excellent creep resistant properties and low flexural modulus.

The mechanism was prototyped using a CNC mill to the specifications listed in Table 3.2 and is shown in Figure 3.9. The unstable equilibrium angle is the angle at which F_{in} becomes negative, or in other words the angle when the device will open unassisted.

3.3.1 Assembly

As Kevlar's chemical composition makes it difficult to bond to metals, a clamping mechanism was employed. The fibers were laid over half the CORE mechanism and a small amount of epoxy (methyl-2-cyanoacrylate) was applied, as a secondary

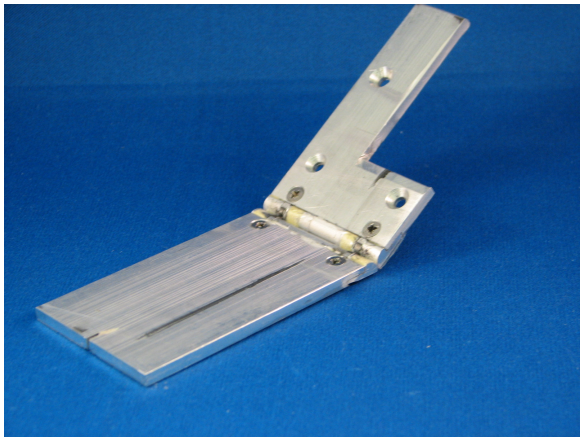

Figure 3.9: Example of the prototyped device used for testing.

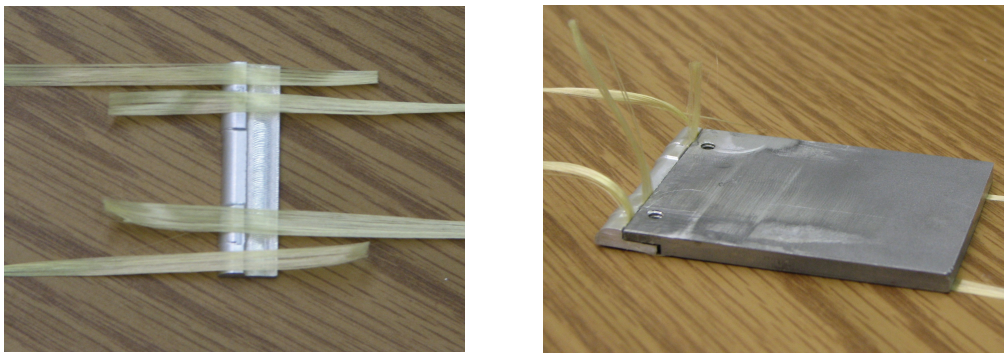

Figure 3.10: Demonstration of clamping method used to secure the Kevlar fibers

method of securing the fibers, to the mechanism just behind the CORE Surface. The remaining half of the mechanism was lowered into place, clamping the fibers to the other half. This piece was secured via 2 screws as shown Figure 3.10.

The fibers were trimmend after assembly to avoid protrusions. This half of the mechanism was then placed into a jig and assembled in the 150° position. During the manufacturing of the device care was taken to remove any surfaces that could damage the Kevlar, such as sharp edges and burrs. Lastly, before the Kevlar was clamped into the mechanism, a small amount of methyl-2-cyanoacrylate was applied to the fibers, further securing the fibers in place.

Table 3.3: Emperical and analytical comparison

Metric	Predicted	Actual	Error
Maximum torque	.122 N/m	.118 N/m	3.2 %
Maximum torque angle	11°	11.727°	6.6%
Unstable Equilibrium Angle	29.5°	30.5°	3.4%

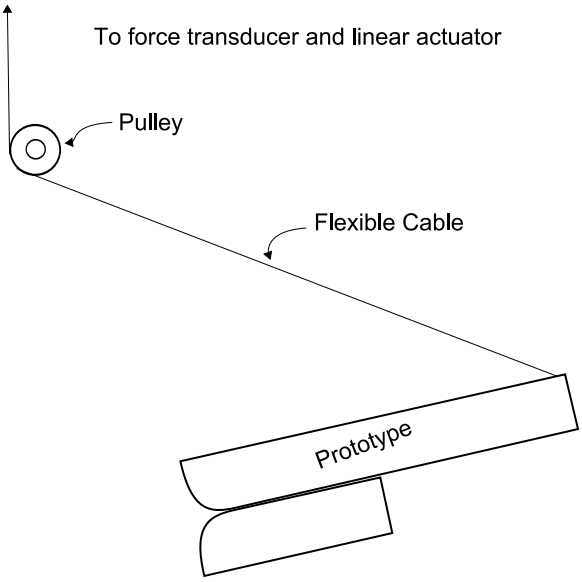

Figure 3.11: Schematic of force measurement setup

3.3.2 Testing

Before beginning the fatigue test the expected and actual results for maximum input torque, maximum input angle torque, and unstable equilibrium angle where compared to the predicted values, the results are shown in table 3.3. The empirical values shown in Table 3.3 were achieved by using the test setup shown in Figure 3.11. A force transducer was rigidly fixed to a linear actuator, a flexible cord was then threaded through a pulley and attached to the prototype, anchored to ground at 15°. Once started the linear actuator displaced the force transducer at a constant rate. The resulting force was obtained using Labview. The moment required to open the prototype was then calculated from the geometry.

All fatigue testing was performed using a custom fatigue testing machine. A Leeson 1 horsepower motor was used to drive a linear sled. The sled held a small ball bearing used to open and close the device, which was secured at an angle of

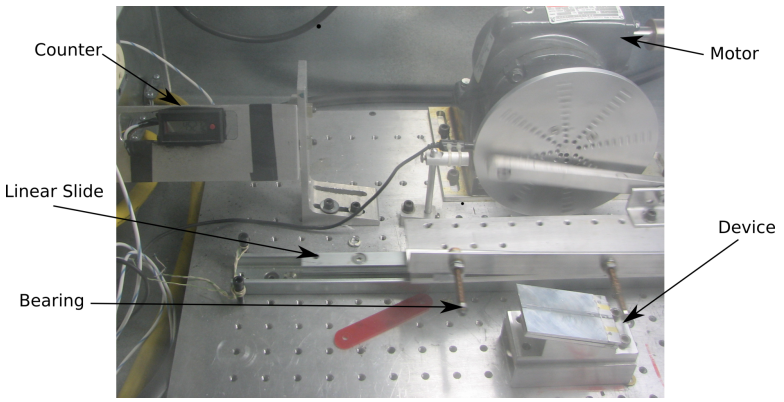

Figure 3.12: Components and setup of fatigue testing equipment

Figure 3.13: Abrasion of Kevlar fibers due to aluminum oxide

15°. The device was rigidly attached to ground. The motor was run at a frequency of 0.75 hertz. This frequency was selected to allow the device to open unassisted (after passing the unstable equilibrium position) and for any vibrations in the upper portion of the device to dampen before the device was closed. The experimental setup is shown in Figure 3.12.

It is interesting to note that the main cause of failure was not due to fatigue of the Kevlar fibers, but due to surface contact fatigue. After several thousand cycles (≈ 2000) a black film (presumably Aluminum Oxide) appeared on the cam surfaces. It was eventually noted that the Aluminum Oxide began to flake and embed itself into the Kevlar fibers. This flaking caused the Kevlar fibers to abraid, see Figure 3.13. To prevent this problem, a small sheath was constructed by folding a thin (0.127 mm)

Figure 3.14: Percent force change with cycling of hinge

mylar sheet and placing it around the Kevlar fibers. This prevented the majority of aluminum oxide from penetrating into the Kevlar, thus extending the life of the mechanism. The force required to open the device, for the sheathed prototypes, was recorded after various cycles, and these results are shown in Figure 3.14.

As Aluminum Oxide forms only on the outer surface (2.54 nm) of Aluminum, it is likely that the degradation of performance was due to the abrasion of the Kevlar and not the reduction in cam surface. Therefore it is believed that an entirely closed sheath, or anodization of the Aluminum, would prevent this degradation.

Chapter 4

Conclusions and Recommendations

4.1 Conclusions

This work has presented seven distinct concepts that, when applied to CORE, will result in multi-stability. Multi-stability may be achieved by placing the CORE flexure into tension or using flexible segments attached to the foci; or by changing the initial curvature of the flexure, curvature of CORE surface, cross sectional area of the flexure (both protagonistically or antagonistically), or material properties. These concepts have expanded the application of CORE mechanisms and have been comparatively scored according to their stability, compactness, number of stable positions, and the likely mode of failure.

These concepts were initially screened using a Pugh scoring matrix and the tension based CORE was determined to be the most promising concept due to its high restoring torque to size ratio. This concept was investigated further and models governing stress, strain, and retaining forces were developed and demonstrated using a case study of a miniature CORE hinge. The case study showed that the CORE hinge performed favorably in fatigue tests and that the failure mode was due to abrasion of the Kevlar fibres.

4.1.1 Applications

While it is expected that a CORE hinge will not be used in every application where traditional pin-in-slot hinges are used today, there are many promising applications for its use. Multi-stable CORE hinges show promising applications in: prosthetic and orthopedic devices, where a reduction in friction and wear is critical; consumer electronics, where electrical connections could be supported; and space

applications, where highly volumetric hinges are disadvantageous due to shipping considerations. Furthermore, the ability of CORE hinges to resist high compressive forces make them useful where typical compliant multi-stable revolute joints would fail, or require inversion.

4.2 Recommendations

4.2.1 Modeling of Bending Stable CORE

During this work, a preliminary investigation of theoretical stability methods were examined. It was noted in this work that the theoretical stabilizing torque differs with the actual torque in bending stable CORE due to the fact that no material is capable of infinite shear stress. Future research is needed in order to understand how the theoretical results differ from those values that are obtained experimentally. Further research should also be conducted into the effect of flexure tension on the overall stability of the mechanism.

4.2.2 Modeling of Tension Stable CORE

Validation of the stress-strain models in CORE should also be investigated. The work conducted during this thesis assumed that the Bernoulli-Euler equation for the bending of a beam was applicable. As stated earlier, one of the assumptions of the Bernoulli-Euler equation is that the material is isotropic; if composite fibres are to be used then an anisotropic model of stress will be necessary. Further design should be performed on the tension stable CORE mechanism to either shield the flexure (i.e. Kevlar fibres) from any fretting that may occur, reduce the amount of fretting that occurs, or both.

Bibliography

[1] C. King, J. J. Beaman, S. Sreenivasan, and M. Campbell, "Multistable equilibrium system design methodology and demonstration," *Journal of Mechanical Design, Transactions of the ASME*, vol. 126, no. 6, pp. 1036 – 1046, 2004

[2] C. W. King, "Design synthesis of multistable equilibrium systems," Ph.D. dissertation, University of Texas at Austin, 2004.

[3] L. L. Howell, *Compliant Mechanisms*. John Wiley & Sons, 2001.

[4] H. Leipholz, *Stability Theory*. Academic Press, New York and London, 1970.

[5] A. G. Erdman and G. N. Sandor, *Mechanism Design: Analysis and Synthesis*, 3rd ed. Prentice Hall, Upper Saddle River, NJ, 1997, vol. 1.

[6] J. E. Shigley and J. J. Uicker, *Theory of Machines and Mechanisms*, 2nd ed. McGraw-Hill, New York, 1995.

[7] B. P. Trease, Y.-M. Moon, and S. Kota, "Design of large-displacement compliant joints," *Journal of Mechanical Design, Transactions of the ASME*, vol. 127, no. 4, pp. 788 – 798, 2005

[8] L. Euler, *Methodus Inveniendi Leneas Curvas Maximi Minimive Peoprietate Gavdentes*. Lausanne and Beneva (Latin), 1744.

[9] R. Cadman, "Rolamite - geometry and force analysis," Sandia Laboratories," Technical report, April 1970.

[10] "Roller-band devices," US Patent 3,452,175, 1967.

[11] N. P. Chironis and N. Sclater, *Mechanisms and Mechanical Devices Sourcebook*. McGraw-Hill, 1996.

[12] J. R. Cannon, C. P. Lusk, and L. L. Howell, "Compliant rolling-contact element mechanisms," *Proceedings of the ASME International Design Engineering Technical Conferences and Computers and Information in Engineering Conference - DETC2005*, vol. 7 A, pp. 3 – 13, 2005.

[13] J. R. Cannon, "Compliant mechanisms to perform bearing and spring functions in high precision applications," Master's thesis, Brigham Young University, 2004.

[14] A. Jeanneau, J. Herder, T. Laliberte, and C. Gosselin, "A compliant rolling contact joint and its application in a 3-dof planar parallel mechanism with kinematic analysis," *Proceedings of the ASME Design Engineering Technical Conference*, vol. 2 A, pp. 689 – 698, 2004.

[15] J. R. Cannon and L. L. Howell, "A compliant contact-aided revolute joint," *Mechanism & Machine Theory*, vol. 40, no. 11, pp. 1273–1293, 2005.

[16] N. D. Mankame and G. Ananthasuresh, "Contact aided compliant mechanisms: Concept and preliminaries," *Proceedings of the ASME Design Engineering Technical Conference*, vol. 5 A, pp. 109 – 121, 2002.

[17] N. D. Mankame and G. K. Ananthasuresh, "Topology optimization of contact-aided compliant mechanisms with smoothened contact modeling," *Computers and Structures*, vol. 82, pp. 1267–1290, 2004.

[18] N. D. Mankame, "Investigations on contact-aided compliant mechanisms," Master's thesis, University of Pennsylvania, 2004.